

Synthesis and Characterization of Some Carbohydrazide Derivatives: Interaction Studies with Human Serum Albumin (HSA), Molecular Docking and Photo-Induced Cleavage

Ahmed Ali Al-Hazmi*, Waddhaah M. Al-asbahy, Faisal Aqlan, Sabah Ahmed Abdo Esmail, Manal Shamsi, Sahar Mansour Al-Sabahi, Labeeb M. Shaif

Department of Chemistry, Ibb University, Ibb, Yemen

Email address

alhazmidrahmed40@gmail.com (A. A. Al-Hazmi)

*Corresponding author

Citation

Ahmed Ali Al-Hazmi, Waddhaah M. Al-asbahy, Faisal Aqlan, Sabah Ahmed Abdo Esmail, Manal Shamsi, Sahar Mansour Al-Sabahi, Labeeb M. Shaif. Synthesis and Characterization of Some Carbohydrazide Derivatives: Interaction Studies with Human Serum Albumin (HSA), Molecular Docking and Photo-Induced Cleavage. *AASCIT Journal of Chemistry*. Vol. 5, No. 1, 2019, pp. 1-13.

Received: October 13, 2018; Accepted: December 3, 2018; Published: April 19, 2019

Abstract: (2E)-3-(furan-2-yl)-1-(pyridin-4-yl)prop-2-en-1-one 1 reacted with 2-cyanoethane-thioamide (2) to afford the corresponding 6'-(2-thienyl)-2'-thioxo-1',2'-dihydro-3,4'-bipyridine-3'-carbonitrile 4. The synthetic potentiality of 4 was investigated through electrophilic substitution reactions using several electrophilic C-species to afford Ethyl {[3'-cyano-6'-(2-thienyl)-3,4'-bipyridin-2'-yl]thio}acetate 5 in very pure state and in a good yield. 3-amino-4-pyridin-3-yl-6-(2-thienyl)thieno[2,3-b]pyridine-2-carbohydrazides (7) was synthesized in good and pure yield *via* the reaction of ethyl {[3'-cyano-6'-(2-thienyl)-3,4'-bipyridin-2'-yl]thio}acetate (5) with hydrazine hydrate. The structures of all newly synthesized heterocyclic compounds were elucidated by considering the data of IR, ¹H NMR, mass spectra as well as that of elemental analyses. In the biological applications, the interaction of compound 7 with human serum albumin (HSA) was investigated under physiological condition in Tris-HCl buffer solution at pH 7.4 by means of various spectroscopic methods (fluorescence, CD and FTIR) and molecular docking technique. The results of fluorescence titration revealed that the compound 7 strongly quench the intrinsic fluorescence of HSA through a static quenching procedure. Binding constants (K_b) and the number of binding sites ($n \approx 1$) were calculated using modified Stern-Volmer equations. The thermodynamic parameters ΔG at different temperatures were calculated subsequently the value of ΔH and ΔS was also calculated which revealed that the hydrophobic and hydrogen bonding interactions play a major role in HSA-compound 7 association. The molecular docking technique was utilized to ascertain the mechanism and mode of action towards the molecular target HSA indicating that compound 7 was located within the subdomain IIA of protein by electrostatic interactions and hydrogen bonds, consistent with the corresponding experimental results. Additionally, compound 7 shows efficient photo-induced HSA cleavage. The results may provide valuable information to understand the mechanistic pathway of drug delivery and to pharmacological behavior of drug.

Keywords: Human Serum Albumin (HSA), Fluorescence Quenching, Molecular Modeling, Carbohydrazide Drugs, Photo-Induced Cleavage

1. Introduction

Carbohydrazide scaffolds is one of the privileged structures in medicinal chemistry. It has wide applications in medicine, environmental protection and explosive materials, which have attracted special attention for their vital role in biological and pharmaceutical activities, such as anticancer,

antibacterial, antifungal antioxidative, and anti-tubercular behavior [1]. The biological activity is dependent upon the compound's structure and its physical-chemical characteristics, as well as the biological entity and its mode of therapeutic treatment [2].

carbohydrazides and similar compounds are well known as useful building blocks for the synthesis of a variety of heterocyclic rings and the carbohydrazide function represents an important pharmacophoric group in several classes of therapeutically useful substances [3, 4].

Human serum albumin (HSA), as the most abundant plasma protein, can bind to a diverse group of endogenous and exogenous compounds [5]. It contains three structurally similar α -helical domains (I–III) that are comprised of sub-domains A and B, which contain six and four α -helices [6], respectively. HSA is a promising drug delivery system because it is non-toxic, non-antigenic, biocompatible and biodegradable and non-immunogenic [7].

The interactions of drugs with protein result in the formation of a stable drug–protein complex, which can exert important effect on the distribution, free concentration and metabolism of the drug in the blood stream. Drugs distribution is mainly controlled by HSA, because most drugs circulate in plasma and reach the target tissues by binding to HSA. Therefore, drug binding to proteins such as HSA has become an important determinant of pharmacokinetics, restricting the unbound concentration and affecting distribution and elimination [8]. Furthermore, affinity of carbohydrazides compounds as drugs towards human serum albumin (HSA) was also investigated since the drug–albumin interaction plays an important role in drug distribution and pharmacokinetics which influences the solubility of the prospective drug, extend its *in vivo* half-life, slow down or prevent its passive extravasations to the target tissues [9].

These studies provide an important rationale for the design of new lead carbohydrazide compound and their specific delivery at the active site of action, besides providing the pharmacological profile *in vitro*.

2. Materials and Methods

2.1. Materials

HSA (fatty acid free, 99%) was purchased from Sigma and used without further purification. All chemicals which used for synthesis compounds were purchased from Sigma, Tris(hydroxymethyl)aminomethane or Tris Buffer (Sigma), were used as received. Doubly distilled water was used as the solvent throughout the experiments. All reagents were of the best commercial grade and used without further purification.

2.2. Sample Preparation

Human serum albumin of 1×10^{-3} M was prepared by dissolving protein in Tris–HCl buffer solution at pH 7.4. The protein concentration was determined spectrophotometrically using an extinction coefficient of $35219 \text{ M}^{-1} \text{ cm}^{-1}$ at 280 nm [10]. Stock solution of compound 7 (1×10^{-3} M) was prepared by dissolving compound 7 in doubly distilled water. NaCl (analytical grade, 1M) solution was used to maintain the ionic strength of buffer at 0.1M pH was adjusted to 7.4 by using HCl. Working standard solution was obtained by

appropriate dilution of the stock solution.

2.3. Apparatus

Shimadzu FTIR–8201PC Spectrophotometer was used for recording IR spectra of KBr pellets in the range of 400–4000 cm^{-1} . The ^1H NMR spectra was obtained on a Varian Mercury 300 MHz spectrometer operating at room temperature. Mass spectra were recorded on Shimadzu GCMS–QP1000EX using an inlet type at 70 eV. Microanalysis of the compounds were obtained on a Carlo Erba Analyzer Model 1108. Emission spectra were recorded with a Hitachi F–2500 fluorescence spectrophotometer. CD spectra were measured on Jasco J–815–CD spectropolarimeter at room temperature.

2.4. Experimental Corrections (Inner Filter Effect)

All fluorescence measurements were corrected for dilution and inner filter effects. Inner filter effects can arise due to either the absorption of the exciting light or by absorption of the emission by the ligands. These corrections were, in all cases, small (>5%) and were estimated for each ligand by the following method. 8×10^{-4} M of a 1×10^{-5} M L-tryptophan solution was added to the same cuvette that had been used for all of the fluorescent quenching experiments. The L-tryptophan solution was titrated with increasing amounts of ligand (drug), and fluorescence intensity measurements were corrected for dilution. The assumption was made that there was no specific interaction between any of the ligands and L-tryptophan and that the reduction in the dilution corrected fluorescent intensity was entirely due to inner filter effects. These data could then be used to correct titrations of HSA with ligand for inner filter effects. 8×10^{-4} M of a 1.8×10^{-4} M L-tyrosine solution was also titrated with each ligand. The data from the titration of L-tyrosine were used to correct titrations of HSA with each ligand for inner filter effects.

2.5. General Procedure for the Synthesis of Carbohydrazide Derivatives

2.5.1. Synthesis of 4 (General Method)

Method A

A solution of 1 (0.43g; 2mmole) and 2 (0.2g; 2 mmole) in absolute ethanol (30 ml) containing a catalytic amount of triethylamine (0.2 ml) was heated under reflux for 5 hours. The reaction mixture then evaporated, cooled, triturated with ethanol. The products so formed collected by filtration, washed with cold ethanol, and then crystallized from the proper solvent to give the corresponding 4.

Method B

A mixture of dispersed sulfur 3 (0.51g; 2 mmole) and morpholine (1.7mL; 2 mmole) in 50 mL of ethanol refluxed for 20 minutes then add malononitrile (0.13g; 2 mmole) and 1 (0.43; 2 mmole) was added and the mixture refluxed for 2 hours. The mixture cooled to $\sim 20^\circ\text{C}$, and 10% HCl added to reach pH 5–6. The precipitates so formed filtered off and

washed with water and cooled ethanol then crystallized from dioxane to give the corresponding 4.

6'-(2-thienyl)-2'-thioxo-1',2'-dihydro-3,4'-bipyridine-3'-carbonitrile (4)

Orange crystals (69%), m.p. 265°C, IR (ν cm⁻¹): 3150 (NH), 3100 (aromatic-CH) and 2250 (CN); MS (z/m) = 295 (100%) which corresponded to formula C₁₅H₉N₃S₂ of the assigned structure as well as m/z = 262 (12.5%) which corresponding to (M⁺ - SH). Anal. for C₁₅H₉N₃S₂ (295.38) Calcd.% C 60.99 H, 3.07 N, 14.23 S, 21.71 Found.% C, 61.76 H, 3.20 N, 14.03 S, 21.01

2.5.2. Synthesis of Ethyl[(3'-cyano-6'-(2-thienyl)-3,4'-bipyridin-2'-yl)thio]acetate (5)

(General Procedure)

A solution of 4 (0.59 g, 2 mmole) and ethyl chloroacetate (0.244 g, 2 mmol) in sodium methoxide (prepared from 0.14 g of sodium and methanol 25 ml) was stirring at room temperature for 15 minutes. The formed precipitate was collected by filtration, washed with water and crystallized from the proper solvent to give 5.

Ethyl {[3'-cyano-6'-(2-thienyl)-3,4'-bipyridin-2'-yl]thio}acetate (5)

Pale yellow crystals (76%), m.p = 145°C; IR (ν cm⁻¹): 3089 (C-H, aromatic), 2220 (CN), 1740 (ester CO); ¹H NMR (DMSO-D₆) (δ ppm): 1.23 (t, 3H, CH₂CH₃), 3.71 (s, 2H, SCH₂), 4.25 (q, 2H, CH₂CH₃), 7.2-8.5 (m, 5H, pyridine H'S) 8.7-9 (m, 3H, thiophene H'S). Anal., for C₁₉H₁₅N₃O₂S₂ (381.47) Calcd.%C, 59.82 H, 3.96 N, 11.02 O, 8.39 S, 16.81 Found.% C, 60.87 H, 3.84 N, 9.95 O, 9.44 S, 15.90

2.5.3. Synthesis of Ethyl 3-amino-4-pyridin-3-yl-6-(2-thienyl)thieno[2,3-b]pyridine-2-carboxylate (6)

Method A

A solution of 5 (0.76g, 2 mmol) in sodium ethoxide solution (prepared from 0.10 g of sodium and 25 mL ethanol) heated under reflux for 30 minutes. The solid that formed after cooling, collected by filtration, washed with water and ethanol then crystallized from the proper solvent to afford 6.

Method B

A solution of 4 (0.59g, 2 mmol) and ethyl chloroacetate (0.244g, 2mmol) in sodium methoxide (prepared from 0.10g of sodium and 25 ml ethanol) heated under reflux for 2 hours. The solid products so formed after cooling, collected by filtration, washed with water and ethanol and dried then crystallized from the proper solvent to afford 6.

Ethyl 3-amino-4-pyridin-3-yl-6-(2-thienyl)thieno[2,3-b]pyridine-2-carboxylate (6)

Yellow crystals crystallized from ethanol (86%); m.p = 245°C; IR (ν cm⁻¹): 3408, 3333 (NH₂), 3057 (C-H aromatic), 1600 (CO); ¹H NMR (DMSO-D₆) (δ ppm): 1.22 (t, 2H, CH₂CH₃), 4.14 (q, 2H, CH₂CH₃), 5.17 (s, 2H, NH₂), 8.7-8.91 and 7.2-8.18 (m, 5H, pyridine H'S) and 8.7-8.91 (m, 3H, thiophene H'S)

Anal, for analysis for C₁₉H₁₇N₃O₂S₂ (381.4): Calcd.% C,

59.33 H, 3.27 N, 15.14 O, 2.47 S, 19.80 Found.% C, 52.09 H, 5.28 N, 19.16 O, 5.49 S, 17.98

2.5.4. Synthesis of 3-Amino-4-pyridin-3-yl-6-(2-thienyl)thieno[2,3-b]pyridine-2-carbohydrazides (7)

Method A

A solution of 5 (0.76g, 2 mmol) in hydrazine hydrate (15mL) and ethanol (20 mL) was heated under reflux for 5 h; the excess solvents were evaporated and cooled. The solid was collected by filtration, dried, and crystallized from the acetic acid to give 7.

Method B

A solution of 6 (0.76g, 2 mmol) in hydrazine hydrate (15mL) and ethanol (20 mL) was heated under reflux for 4 h; the excess solvents were evaporated and cooled. The solid was collected by filtration, dried, and crystallized from the acetic acid to give 7.

3-Amino-4-pyridin-3-yl-6-(2-thienyl)thieno[2,3-b]pyridine-2-carbohydrazide (7)

Yellow crystals (90%), m.p. = 290°C; IR (ν cm⁻¹): 3463, 3320, 3301, 3230 (NH & NH₂), 3044 (aromatic-CH); and CONH was shown at (1600) MS: 367 (M⁺, 34.3% which corresponding to the molecular weight of the molecular formula C₁₇H₁₃N₅O₁S₂ of the assigned structure), 336 (M⁺-NHNH₂, 100%); 308 (M⁺-CONHNH₂, 7.4%); ¹HNMR (DMSO-D₆) (δ ppm): 5.18 (br, s, 2H, NH₂); 6.2 (t, 2H, NH₂); 7.202- 9 (m, 8H, pyridinyl H's, thiophene H's); 10.2 (1H, NH) Anal, for C₁₇H₁₃N₅O₁S₂ (367) Calcd.% C, 55.57 H, 3.57 N, 19.06 O, 4.35 S, 17.45 Found.% C, 52.17 H, 6.28 N, 18.26 O, 5.39 S, 17.90.

2.6. HSA-Binding Experiments

2.6.1. UV-Visible Spectroscopy

Absorption spectra were recorded on a Shimadzu UV-1800 pharmaspec UV-Vis spectrophotometer using cuvettes of 1 cm path length. HSA concentration was determined from absorption spectra, taking the absorbance of a 1x10⁻³ M solution at 280 nm (λ_{maxTrp} -214) as 1.80 x 10⁻⁶ M. The value of binding constants can be calculated from the method which was described earlier [11]. By assuming that there is only one type of interaction between compound 7 and HSA in aqueous solution, eqn (1) and (2) can be established:

$$[HSA]+[compound\ 7]\leftrightarrow[HSA:Compound\ 7] \quad (1)$$

$$K = \frac{[HSA:compound\ 7]}{[HSA][compound\ 7]} \quad (2)$$

where K is the binding constant for Compound 7

Assuming $[HSA:Compound\ 7] = C_B$

$$K = \frac{C_B}{(C_{HSA}-C_B)(C_{compound\ 7}-C_B)} \quad (3)$$

where C_{HSA} and Compound 7 are analytical concentration of HSA and compound 7 in the solution, respectively.

According to the Beer-Lambert law

$$C_{HSA} = \frac{A_0}{\varepsilon_{HSA}l} \quad (4)$$

$$C_B = \frac{A-A_0}{\varepsilon_{HSA}l} \quad (5)$$

where A_0 and A are the absorbance of HSA at 280 nm, in the absence and presence of compound 7, respectively. ε_{HSA} and ε_B are the molar extinction coefficient of HSA and the bound compound 7, respectively, and l is the light path of the cuvette (1cm). By substituting ε_{HSA} and ε_B in eqn (4) and (5) in eqn (3), the equation can be deduced as follows:

$$\frac{A_0}{A-A_0} = \frac{\varepsilon_{HSA}}{\varepsilon_B} + \frac{\varepsilon_{HSA}}{\varepsilon_B K} \frac{1}{C_{\text{Compound 7}}} \quad (6)$$

Thus, the double reciprocal plot of $1/A-A_0$ vs. $1/C_{\text{compound 7}}$ is linear and the binding constant can be estimated from the ratio of the intercept to the slope.

2.6.2. Fluorescence Quenching

Fluorescence measurements were carried out on Hitachi F-4500 fluorescence spectrophotometer in a 1 cm path-length quartz cell with the excitation and emission wavelength set at 280 and 300–400 nm, respectively. The interaction of compound 7 ($0.33\text{--}2 \times 10^{-5}$ M) with HSA content of fixed concentration (1.00×10^{-5} M) was studied. The intensity at 350 nm (Tryptophan) was used to calculate the binding constant (K). The fluorescence quenching of HSA at different temperatures (298, 308 and 318 K) were determined using the Stern–Volmer equation [12]:

$$\frac{F_0}{F} = 1 + k_q \tau_o [Q] = 1 + K_{sv} [Q] \quad (7)$$

where F_0 and F are the fluorescence intensities in absence and presence of quencher, respectively, $[Q]$ is the quencher concentration, and K_{sv} Stern–Volmer quenching constant, which can be written as

$$k_q = \frac{K_{sv}}{\tau_o} \quad (8)$$

where k_q is the biomolecular quenching rate constant and τ_o is the average lifetime of the fluorophore (Trp-214) in absence of quencher and its value is around 10^{-8} s for most biomolecules [13]. Therefore, Eq. (9) was applied to determine K_{sv} by linear regression of a plot of F_0/F vs $[Q]$.

2.6.3. Calculation of Binding Constant

The binding constant was calculated from the modified Stern–Volmer equation (Eq. (9))

$$\frac{1}{[F_0 - F]} = \frac{1}{F_0} + \frac{1}{K_b} \frac{1}{F_0} \frac{1}{Q} \quad (9)$$

where K_b is the binding constant of compound 7 with biomolecule which was calculated from the intercept and slope of the Lineweaver–Burk ($1/(F_0 - F)$ versus $1/[Q]$) (intercept = $1/F_0$, slope = $1/K_b F_0$, so K_b = intercept/slope).

Furthermore, the binding constant (K) and number of bound compound 7 to HSA (n) were determined by plotting the double log graph of the fluorescence data using (Eq. (10)).

$$\log \left[\frac{F_0 - F}{F} \right] = \log K + n \log [Q] \quad (10)$$

2.6.4. Determination of Thermodynamic Parameters

The thermodynamic parameters were calculated from the van't Hoff equation (Eq. (11))

$$\ln K = \frac{-\Delta H}{RT} + \frac{\Delta S}{R} \quad (11)$$

where K is the Lineweaver–Burk static quenching constant at corresponding temperature and R is the gas constant, in which ΔH and ΔS of reaction was determined from the linear relationship between $\ln K$ and the reciprocal absolute temperature. Furthermore, the free energy change (ΔG) was calculated by the Eq. (12).

$$\Delta G = \Delta H - T\Delta S = -RT \ln K \quad (12)$$

2.6.5. Calculations of Energy Transfer

According to Förster resonance energy transfer (FRET), the efficiency of energy transfer (E) is given by [14]:

$$E = 1 - \frac{F}{F_0} = \frac{R_0^6}{R_0^6 + r_o^6} \quad (13)$$

where F and F_0 are the fluorescence intensities of HSA in the presence and absence of quencher, r is the distance between acceptor and donor and R_0 is the critical distance when the transfer efficiency is 50%. The value of R_0 was calculated using the Eq. (14):

$$R_0^6 = 8.78 \times 10^{-25} k^2 N^{-4} \phi J \quad (14)$$

where k^2 is spatial orientation factor between the emission dipole of the donor and the absorption dipole of acceptor, N is the refractive index of the medium, ϕ is the fluorescence quantum yield of the donor and J is the overlap integral of the fluorescence emission spectrum of the donor and the absorption spectrum of the acceptor and calculated by Eq. (15):

$$J = \frac{\sum F(\lambda) \varepsilon(\lambda) \lambda^4 \Delta \lambda}{\sum F(\lambda) \Delta \lambda} \quad (15)$$

where $F(\lambda)$ is the corrected fluorescence intensity of the donor at wavelength λ and $\varepsilon(\lambda)$ is the molar absorption coefficient of the acceptor at wavelength λ . Under the experimental condition, the value of $K^2 = 2/3$, $N = 1.336$, and $\phi = 0.188$ [15].

2.6.6. Circular Dichroism (CD) and Fourier Transform Infrared (FTIR) Measurements

CD spectra were measured on Jasco J-815-CD

spectropolarimeter (Jasco, Japan) at room temperature using a 1 cm quartz cuvette. Measurements were taken at wavelengths between 200 and 250 nm. All observed CD spectra were baseline subtracted for buffer and the CD results were expressed in terms of MRE (mean residue ellipticity) in $\text{deg cm}^2 \text{d mol}^{-1}$ as Eq. (16):

$$MRE = \left[\frac{\text{Observed CD (m deg)}}{C_p n l \times 10} \right] \quad (16)$$

where C_p is the molar concentration of the protein, n the number of amino acid residues (585) and l the path length (0.1 cm). The α -helical contents of free and combined HSA were calculated from the MRE value at 208 nm using the Eq. (17) as described by Lu *et al.* [16]:

$$\alpha\text{-helix(\%)} = \left[\frac{-(MRE)_{208} - 4000}{33000 - 4000} \right] \times 100 \quad (17)$$

where MRE_{208} is the observed MRE value at 208 nm, 4000 is the MRE of the β -form and random coil conformation cross at 208 nm, and 33000 is the MRE value of a pure α -helix at 208 nm.

Fourier Transform Infrared measurements carried out on an Interspec 2020 FTIR spectrometers were recorded in liquid phase in 400–4000 cm^{-1} range at room temperature, with a Germanium attenuated total reflection (ATR) accessory, a DTGS KBr detector and a KBr beam splitter. All spectra were taken via the Attenuated Total Reflection (ATR) method with resolution of 4 cm^{-1} and 60 scans. The spectra processing procedure involved collecting spectra of buffer solution under the same conditions. Next, the absorbance of the buffer solution was subtracted from the spectra of the sample solution to obtain the FT-IR spectra of the protein. The subtraction criterion was that the original spectrum of the protein solution between 2200 and 1400 cm^{-1} was featureless [17].

2.6.7. HSA Photo-Cleavage Studies

Photo-induced protein cleavage experiments were performed following to the standard methods according to the literature [18]. The photo-induced protein cleavage studies were carried out using incubating HSA in 50 mM Tris-HCl buffer (pH 7.4). The protein solutions (15 μM) containing compound 7 with increasing concentrations 100 to 250 μM were photo-irradiated at 365 nm for 4 h incubation at 37 °C followed by SDS-PAGE analysis.

2.6.8. Molecular Docking

The rigid molecular docking studies were performed by using HEX 6.1 software [19], is an interactive molecular graphics program to understand the drug-protein interaction. The Structure of the compound was sketched by CHEMSKETCH (<http://www.acdlabs.com>) and converts it into pdb format from mol format by OPENBABEL (<http://www.vclab.org/lab/babel/>). The crystal structure of

the human serum albumin (PDB ID: 1h9z) was downloaded from the protein data bank (<http://www.rcsb.org/pdb>). All calculations were carried out on an Intel Pentium 4, 2.4 GHz based machine running MS Windows XP SP2 as operating system. Visualization of the docked pose has been done by using PyMol (<http://pymol.sourceforge.net/>) molecular graphic program.

3. Results and Discussion

3.1. Synthesis and Characterization

(2*E*)-3-pyridin-3-yl-1-(2-thienyl)prop-2-en-1-one(1) reacted with 2-cyanoethane thioamide (2) in absolute ethanol containing acatalytic amount of triethylamine under reflux to afford a reaction product. Such reaction product formed *via* a Michael addition of $-\text{CH}_2-$ in 2 on $-\text{CH}=\text{CH}-$ of 1 to give the non-isolable products followed by cyclisation *via* dehydration and dehydrogenation to give 4. The IR (cm^{-1}) of this reaction product showed the bands of NH (3150) and CN (2250) groups. Its mass spectrum gave $m/z = 295$ (100%) which corresponding to the molecular weight of the molecular formula $\text{C}_{15}\text{H}_9\text{N}_3\text{S}_2$ of the assigned structure as well as $m/z = 262$ (12.5%) which corresponding to (M^+ , -SH) (Figure 1).

A further confirmation of 4 arose from their synthesis through other pathway *via* the reaction of each of 1 and malononitrile in a dispersed sulfur (3), morpholine and ethanol under reflux 2 hours. It important to refer here that 4 obtained by the two pathways are identical in allphysical and chemical properties (Figure 1).

The synthetic potentiality of 4 was investigated through electrophilic substitution reactions using several electrophilic C-species. Thus, it has been found that 4 was reacted with ethylchloroacetate in stirred methanolic sodium methoxide at room temperature for 15 minutes to give a reaction product. The IR (cm^{-1}) of this reaction product showed the bands of CN (2220) and CO (1740) of the newly introduced COOEt group. Its ^1H NMR (δ ppm) spectrum revealed the signals of $-\text{SCH}_2-\text{COOCH}_2\text{CH}_3$, $-\text{COOCH}_2\text{CH}_3$ protons and this confirm the good nucleophilicity of S in 4 that facilitate the electrophilic attack of C at ethylchloroacetate to afford 5 in very pure state and in a good yield. Furthermore, 5 structure elucidated through its cyclization in ethanolic sodium ethoxide under reflux for 30 minutes to give a reaction product whose IR spectrum showed no bands of CN group and instead the bands of the newly formed NH_2 group detected. Also, the ^1H NMR spectrum of this reaction product revealed no signals of $-\text{SCH}_2-$ protons while that of NH_2 detected. The data of both IR and ^1H NMR were concluded that both $-\text{SCH}_2-$ and CN functional groups in 5 involved in the cyclisation step to give the finally isolated 6. A further confirmation of 6 structure obtained through its preparation authentically *via* the reaction of 4 with ethylchloroacetate in ethanolic sodium ethoxide under reflux for 2 hours (Figure 2).

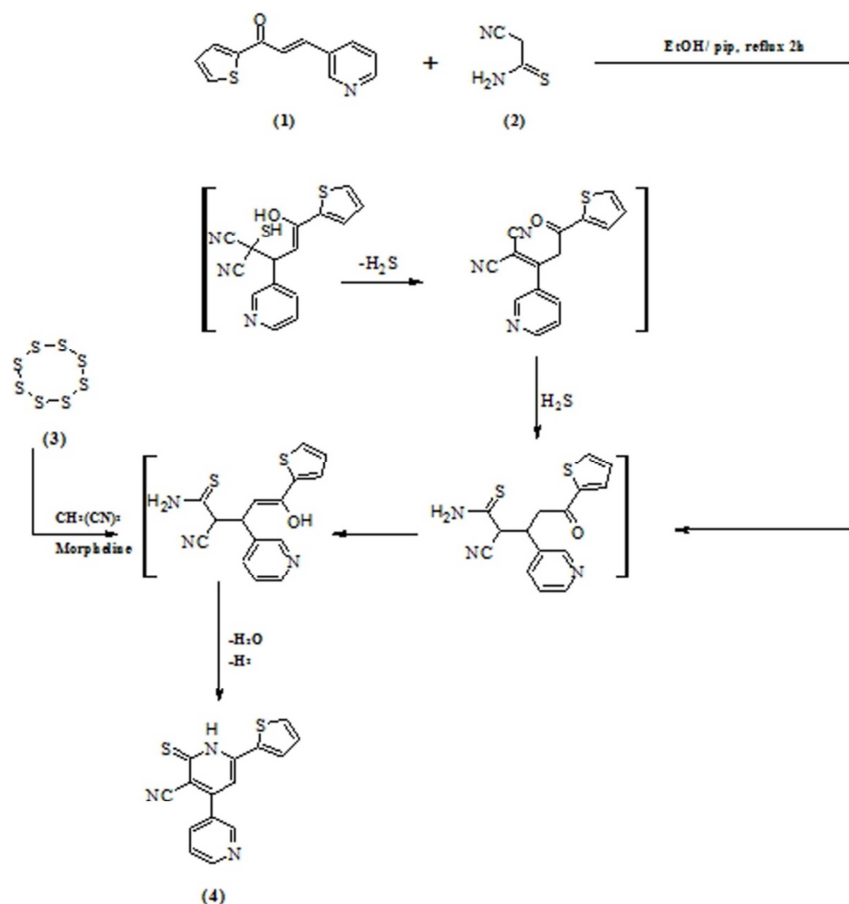


Figure 1. Synthesis of the newly Carbohydrazide derivatives (1–4).

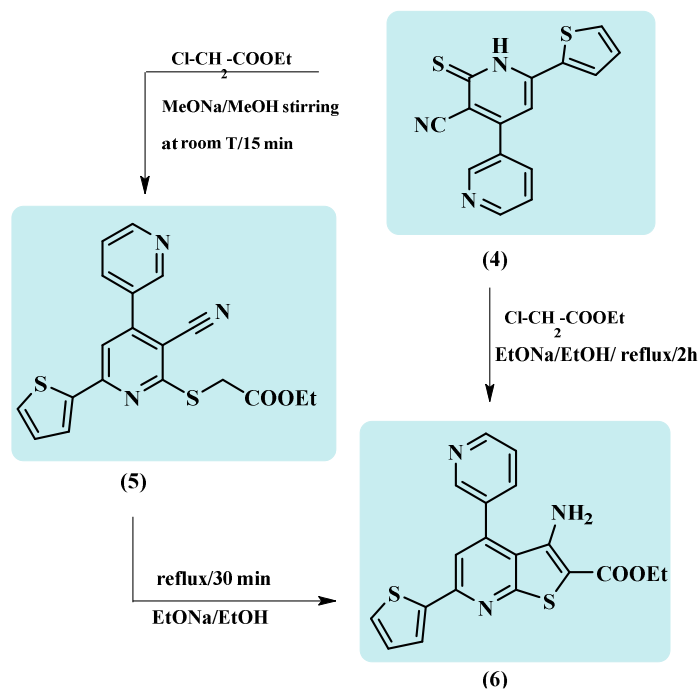


Figure 2. Synthesis of the newly Carbohydrazide derivatives (4–6).

3-amino-4-pyridin-3-yl-6-(2-thienyl)thieno[2,3-*b*]pyridine-2-carbohydrazides (7) was synthesized in good and pure yield *via* the reaction of ethyl {[3'-cyano-6'-(2-

thienyl)-3,4'-bipyridin-2'-yl]thio}acetate(5) with hydrazine hydrate under reflux for 3–5 hours. The IR (cm^{-1}) of this reaction product showed no bands for CN and CO functions

while the newly formed NHNH_2 functions detected (cf. Exp. Part).

Thus, the reaction has more probably proceeded *via* the nucleophilic attack of the hydrazine N atom on the electrophilic C of the COOEt group followed by both removal of ethanol molecule and intramolecular cyclization to afford 7. The structure of 7 was further confirmed chemically by its preparation authentically *via* reaction of

ethyl 3-amino-4-pyridin-3-yl-6-(2-thienyl)thieno[2,3-*b*]pyridine-2-carboxylate (6) with hydrazine hydrate. Mass spectrum used as a physical tool to elucidate 7 structure where it gave peaks at $m/z=367$ (34.3%) which corresponding to the molecular weight of the molecular formula $\text{C}_{17}\text{H}_{13}\text{N}_5\text{O}_1\text{S}_2$ of the signed structure; $m/z=336$ (100%, M^+ , $-\text{NHNH}_2$); 308 (7.4%, $\text{M}^+-\text{CONHNH}_2$) (Figure 3).

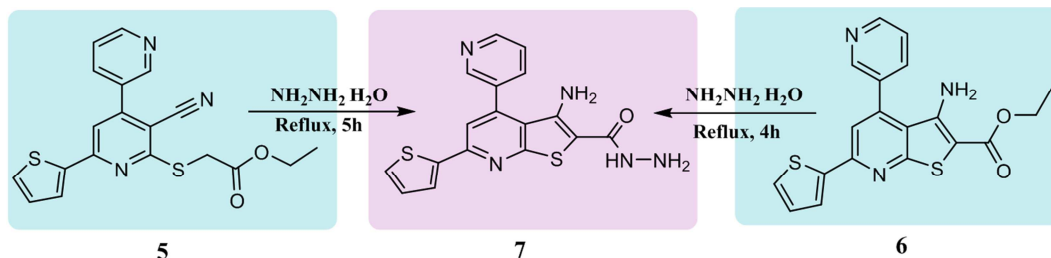


Figure 3. Synthesis of the compound (7).

3.2. HSA Binding Studies

3.2.1. *In Vitro* Binding Studies with HSA

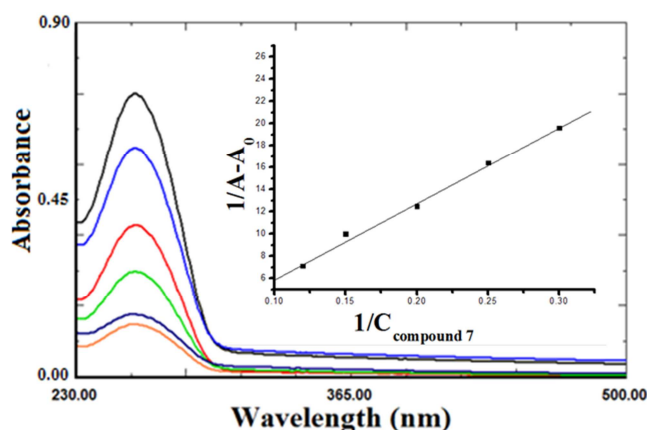


Figure 4. UV absorption spectra of the HSA–compound 7 conjugate system obtained in 5 mM Tris–HCl/50 mM NaCl buffer, pH 7.4, at room temperature: (a) HSA, 1.00×10^{-5} M; (b–f) compound 7–HSA, the compound 7 concentrations were $0.00\text{--}2.33 \times 10^{-5}$ M, respectively.

The efficiency of a drug is greatly influenced by the degree to which it binds to proteins within the blood plasma. The less bound a drug is, the more efficiently it can traverse through cell membranes. The absorption spectral studies were employed to investigate the binding strength and the conformational structure changes of HSA with compound 7. Upon the addition increasing concentration of compound 7 ($0\text{--}4.0 \times 10^{-5}$ M) to a fixed concentration of HSA (1.0×10^{-5} M), there was a sharp increase in absorption peak at ~ 280 nm attributed to the aromatic rings in tryptophan (Trp-214), tyrosine (Tyr-411) and phenylalanine (Phe) residues in HSA (Figure 4). The observed “hyperchromism” suggested the involvement of non-covalent interactions most likely by electrostatic attraction between the compound 7 and HSA. To assess the binding ability of the compound 7 with HSA, the intrinsic binding constant (K_b) value was calculated and found to be $3.84 \times 10^4 \text{ M}^{-1}$. The K_b values suggest that

compound 7 has a strong binding affinity for HSA, followed by conformational changes in its structure, which is further validated by the circular dichroism spectroscopy and the molecular docking technique.

Since strong affinity of a drug towards a protein helps in the diffusion of the drug from the circulatory system to reach its target site, thus obtained K_b value for compound 7 fulfill this criterion for their transport in the blood circulation and diffusion at the target site.

3.2.2. Fluorescence Quenching of HSA by Compound 7

Fluorescence spectroscopy, which is a sensitive technique for investigating the microenvironment of amino acid residues, and also its suitable tool for monitoring interactions between drugs and macro-biomolecules [20]. Fluorescence quenching refers to any process which decreases the fluorescence intensity of a sample such as excited state reactions, energy transfers, ground-state complex formation and collisional process [21]. It is well known that there are two quenching mechanisms involved in quenching process, which are usually classified as dynamic quenching and static quenching. The fluorescence properties of HSA arise from the intrinsic characteristic of protein, mainly due to presence of tryptophan residue (Trp-214). Fluorescence spectral studies were performed by using 1.0×10^{-5} M HSA and various the concentration of compound 7 ($0.0\text{--}2.0 \times 10^{-5}$ M) is shown in Figure 5a, when the excitation wavelength (λ) was 280 nm, HSA had a strong fluorescence emission peak at 350 nm, fluorescence was not observed in the compound 7 or buffer solution under the present experimental conditions.

The fluorescence intensity of human serum albumin (HSA) decreased gradually with the addition of compound 7, which indicated that the compound 7 bound to HSA. To have a deep insight into the fluorescence quenching mechanism, quenching experiments were performed at three different temperatures viz., 298, 308 and 318 K.

In order to ascertain the fluorescence quenching mechanism, the fluorescence quenching data at different

temperatures (298, 308 and 318 K, Figure 5b) were analyzed using the classical Stern–Volmer equation. The results (Table 1) showed that the Stern–Volmer quenching constant K_{sv} is inversely correlated with temperature, and the values of kq being larger than the limiting diffusion constant K_{dif} of the

biomolecule ($K_{dif} = 2.0 \times 10^{10} \text{ M}^{-1}\text{s}^{-1}$), suggested that the fluorescence quenching was caused by a specific interaction between HSA and compound 7 occurred *via* static quenching mechanism through the formation of a complex.

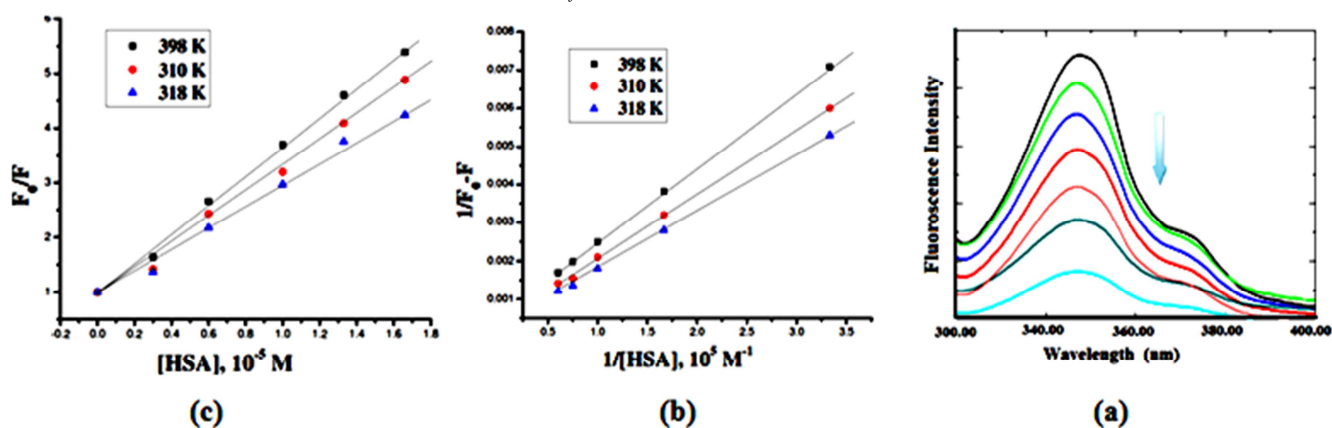


Figure 5. (a) Fluorescence quenching spectra of HSA ($1.0 \times 10^{-5} \text{ M}$) by different concentrations of compound 7 corresponding to $0.00\text{--}2 \times 10^{-5} \text{ M}$ with the excitation wavelength at 280 nm in 5 mM Tris-HCl/50 mM NaCl buffer, pH 7.4, at room temperature. Arrow shows the intensity changes upon increasing concentration of the quencher. (b) Stern–Volmer plots showing HSA tryptophan quenching caused by compound 7 at three different temperatures. (c) Lineweaver–Burk plot for the binding of HSA with compound 7 at different temperatures.

3.2.3. Number of Binding Sites

For the static quenching process, the quenching data were analyzed according to the modified Stern–Volmer equation (Eq. (9)). As shown in Figure 6a, the binding constant decreased with increasing temperature (see Table 1), which coincided with the Stern–Volmer quenching constant. As static quenching, the quenching constant can be interpreted as the association constant of the compound reaction since static quenching occurs from the formation of a ground state compound which is non-fluorescent or weakly fluorescent between fluorophore and quencher.

Table 1. Stern–Volmer quenching constant of the compound 7–HSA system at different temperatures.

pH	T(K)	$K_{sv}(10^5\text{M}^{-1})$	$k_q(10^{13}\text{M}^{-1}\text{s}^{-1})$	R
7.40	298	1.98	1.98	0.999
	308	1.69	1.69	0.998
	318	1.51	1.51	0.999

When small molecules bind independently to a set of equivalent sites on a macromolecule, the equilibrium between free and bound molecules is given by the Eq. 10.

The number of binding sites (n) were calculated ~ 1 at different temperatures, which strongly supported the existence of a single binding site in HSA for compound 7 (Table 2). Meanwhile, the binding constants between compound 7 and human serum albumin decreased with increasing temperature, which indicated that high temperature reduced the binding affinity of human serum albumin and compound 7. This indicated that tyrosine residues and tryptophan residues were both involved in the

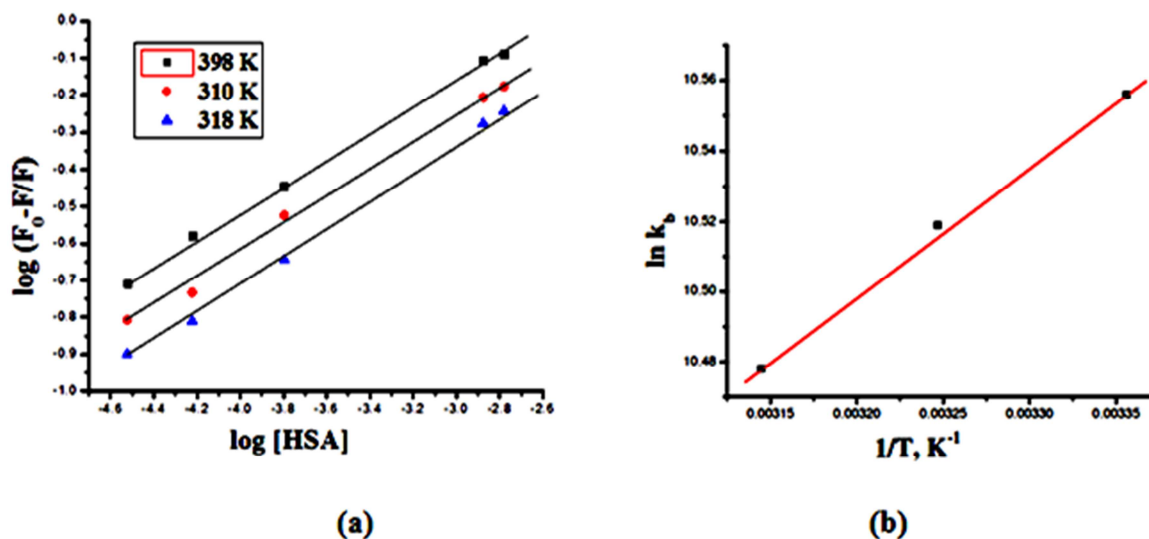
interaction of human serum albumin and compound 7.

3.2.4. Thermodynamic Parameters and Nature of the Binding Forces

The interacting molecular forces between compound 7 and HSA exhibit weak interactions such as electrostatic forces, hydrophobic interaction, hydrogen–bond formation, van der Waals forces and stereo–hindrance effect, etc. [22]. The thermodynamic parameters, enthalpy change (ΔH), entropy change (ΔS) and free energy change (ΔG) are the main evidence for confirming the binding modes. From the thermodynamic standpoint, $\Delta H > 0$ and $\Delta S > 0$ implies a hydrophobic interaction; $\Delta H < 0$ and $\Delta S < 0$ reflects the van der Waals force or hydrogen bond formation; and $\Delta H \approx 0$ and $\Delta S > 0$ suggests an electrostatic force. The positive ΔS value is frequently taken as evidence for hydrophobic interaction. Furthermore, the negative ΔH value observed cannot be mainly attributed to electrostatic interactions since for electrostatic interactions ΔH is very small, almost zero. A negative ΔH value is observed when ever there is hydrogen bond on the binding site [23]. It is not possible to account for the thermodynamic parameters of the compound 7–HSA coordination compound on the basis of a single intermolecular force. Consequently, the negative ΔH (-21.72 KJ/mole) and positive ΔS ($+111.55 \text{ J/mole K}$) values suggest that hydrophobic and hydrogen bond interactions play major roles in the compound 7–HSA binding reaction and contributed to the stability of the compound. The negative value of ΔG reveals that the interaction process is spontaneous (Figure 6b and Table 2).

Table 2. Binding constant (K_b), the number of binding sites (n) and ΔG values for the compound 7–HSA system at different temperatures.

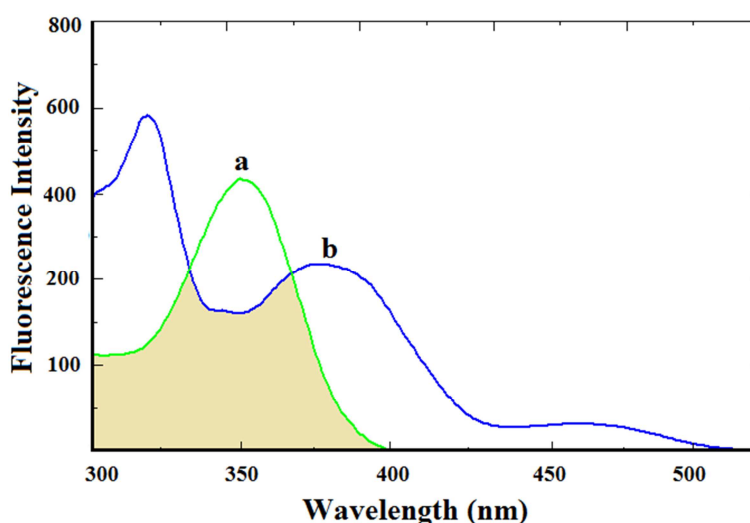
pH	T(K)	$K_b(10^4 M^{-1})$	n	$\Delta G(kJ/mole)$	$\Delta H(kJ/mole)$	$\Delta S(J/mole.K)$
7.40	298	3.842	0.97	-11.358	-21.72	+111.55
	308	3.701	1.01	-11.698		
	318	3.553	0.99	-11.133		

**Figure 6.** (a) Logarithmic plot of the fluorescence quenching of HSA at different temperatures, (b) Van't Hoff plot for the interaction of compound 7 and HSA.

3.2.5. Energy Transfer Between Compound 7 and HSA

Fluorescence energy transfer occurs *via* overlapping of emission spectrum of a fluorophore (donor) overlaps with the absorption spectrum of another molecule (acceptor). The overlap of the absorption spectrum of the compound 7 with the fluorescence emission spectra of free HSA is shown in Figure 7. The rate of energy transfer depends on: (i) the extent of overlapping between fluorescence emission spectrum of donor and the absorption spectrum of acceptor, (ii) the relative orientation of the donor and acceptor dipoles,

and (iii) the distance between the donor and the acceptor. Here the donor and acceptor were HSA and the compound 7, respectively. From Eqs. (14)–(15), the value of E , R_0 , r and J were calculated and found to be 0.89, 2.86 nm, 4.1 nm and $1.63 \times 10^{-14} M^{-1} cm^3$, respectively. The donor to acceptor distance $r < 7$ nm indicated that the energy transfer from tryptophan residue in HSA to compound 7 occur with high probability [24]. Which is also in accordance with the conditions of FRET, indicating the static quenching interaction between compound 7 and HSA.

**Figure 7.** (a) The overlap of UV absorption spectra of compound 7 with the fluorescence emission spectra of HSA. (a) The fluorescence emission spectrum of HSA ($1.0 \times 10^{-6} M$); (b) the UV absorption spectrum of compound 7 ($1.00 \times 10^{-5} M$).

3.2.6. Changes of the Protein's Secondary Structure Induced by Compound 7

To ascertain the possible influence of compound 7 binding on the secondary structure of HSA, CD measurement was performed in the presence of compound 7 at different concentrations. As shown in Figure 8, CD spectra of free HSA (line a) exhibit two negative bands in the ultraviolet region at 208 and 222 nm are contributed to $n \rightarrow \pi^*$ transfer for the peptide bond of α -helix [25]. It was observed that in presence of compound 7 the CD signal of HSA increased. The increase of the CD signal indicates decrease of helical secondary structure content. This phenomenon is like with the interaction of HSA with compound 7. However, the CD spectra of HSA in the presence or absence of compound 7 is similar in shape, indicating that the structure of HSA is also predominantly α -helical. From above Eqs 16 and 17, the quantitative analysis results of the α -helix in the secondary structure of HSA were obtained. They differed from that of 56.88% in free HSA to 48.43% in the compound 7-HSA conjugate at pH 7.4 and temperature 298K. The α -helix gradually decreases in presence of compound 7, which reveals that the interaction between compound 7 and HSA

leads to a change of the protein's secondary structure [26].

To further understand the structural alternations of HSA induced by the binding of compound 7 to HSA, FT-IR spectroscopy were performed on HSA and compound 7-HSA system (Figure 9a and b). The spectrum in Figure 9(a) was obtained by subtracting the absorption of the Tris-HCl from the spectrum of the protein solution. The spectrum in Figure 9(b) was obtained by subtracting the absorption of the compound 7-free form from that of the compound 7-bound form. Infrared spectra of proteins exhibit a number of the amide bands, which represent different vibrations of the peptide moiety. Among these amide bands of the protein, amide I peak position occur in the range $1600\text{--}1700\text{ cm}^{-1}$ (mainly C=O stretch) and amide II band in the region $1500\text{--}1600\text{ cm}^{-1}$ (C-N stretch coupled with N-H bending mode). The amide bands have a relationship with the secondary structure of protein, and amide I is more sensitive than amide II for change of secondary of protein [27]. As shown in Figure 9, the peak position of amide I band was shifted from 1644.9 cm^{-1} to 1638.7 cm^{-1} , implicating that that the secondary structure of the HSA protein altered due to interaction of compound 7.

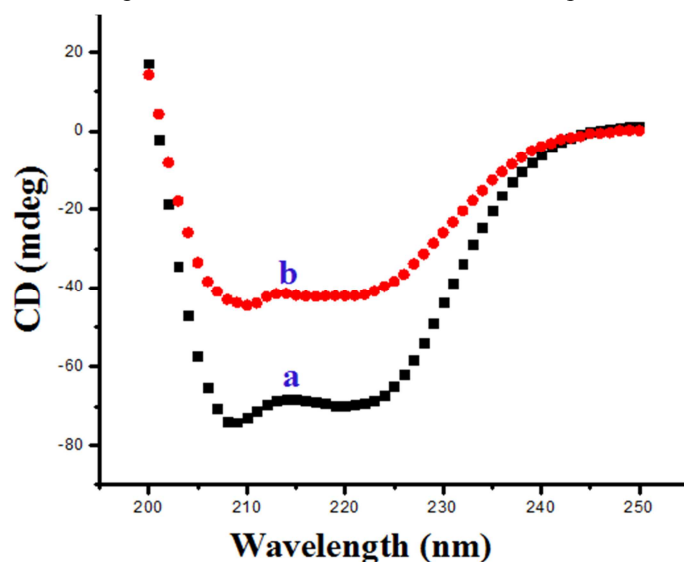


Figure 8. CD Spectra of the HSA-compound 7 conjugate. (a) $1.0 \times 10^{-5}\text{ M}$ HSA; (b) $1.0 \times 10^{-5}\text{ M}$ HSA + $1.5 \times 10^{-5}\text{ M}$ compound 7.

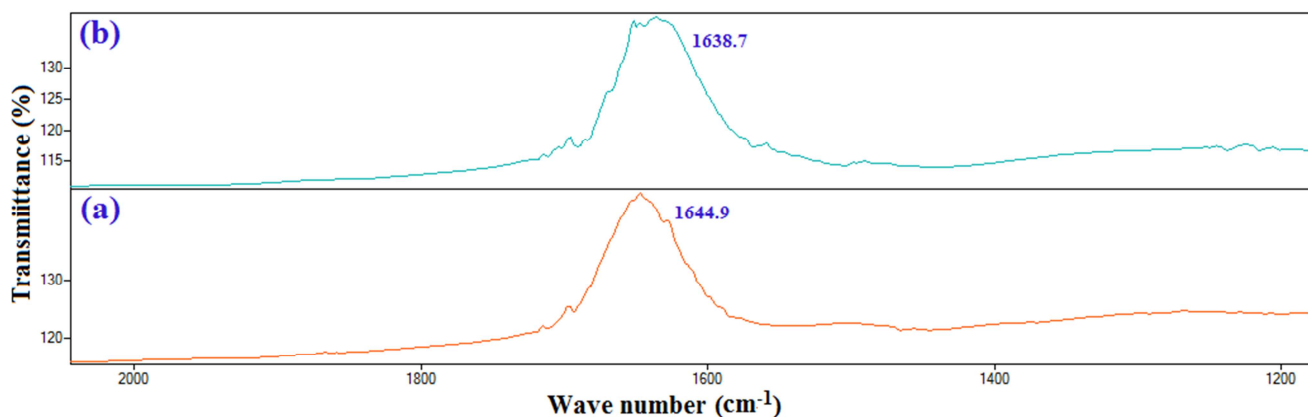


Figure 9. FT-IR spectra of (a) free HSA; (b) different spectra [(HSA solution + compound 7 solution) - (compound 7 solution)] in 5 mM Tris-HCl/50 mM NaCl buffer, pH 7.4, at room temperature in the region of $1750\text{--}1400\text{ cm}^{-1}$, [HSA], $1.0 \times 10^{-5}\text{ M}$; [compound 7], $1.5 \times 10^{-5}\text{ M}$.

3.2.7. HSA Photo-Cleavage Studies

To investigate the ability of compound 7 to photo-induced degradation of HSA induced by controlling the wavelength of excitation, specific chromophores can be selectively activated to high energies, thereby minimizing side reactions [28]. Such chemical proteases can be utilized for breaking large proteins into smaller fragments that are more amenable to sequencing. The ability of compound 7 to mediate protein cleavage is well established in literature [29].

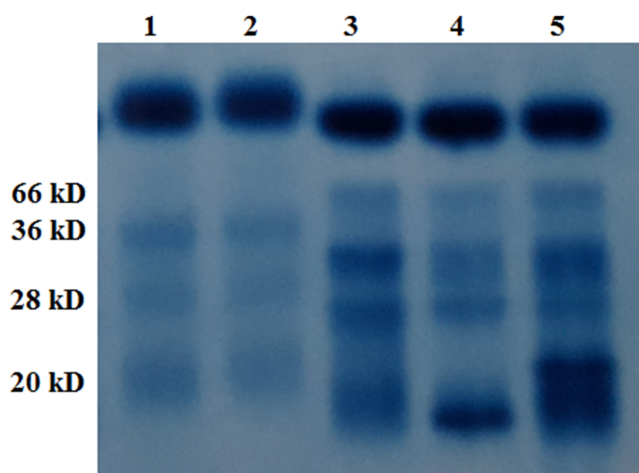


Figure 10. SDS-PAGE electrophoresis in 12% polyacrylamide gel showing photocleavage of human serum albumin (HSA, 15 μ M) with 20 min photoexposure to UV-A1 light at 365 nm by the compound 7 in Tris HCl buffer (pH 7.4), (a) at different concentration; lane-1, HSA control (molecular size marker); lane-2, HSA + compound 7 (50 μ M); lane-3, HSA + compound 7 (100 μ M); lane-4, HSA + compound 7 (150 μ M); lane-5, HSA + compound 7 (200 μ M, in dark).

In order to ascertain the ability of the compound 7 to serve as a synthetic chemical proteases, the HSA photo-cleavage activity of the compound 7 was studied using 15 μ M HSA in 50 mM Tris-HCl buffer on exposure to UV-A1 light of 365 nm with different drug concentrations for 20 min and the extent of cleavage was compared with the untreated HSA band. The photo-induced protease activity of compound 7 was assayed by SDS-PAGE (12%) analysis. As shown in Figure 10, it was observed that HSA alone (Lane 1) did not show any apparent cleavage under these conditions. However, upon increasing the concentration of compound 7 (100–200 μ M), HSA showed significant smearing or fading of the band (Lane 2–6), indicating photo-cleavage of HSA under physiological reaction conditions. At the same time, when the concentration of compound 7 reached to 150 μ M, HSA cleaved into smaller fragment that can be observable by SDS-PAGE due to cleavage of HSA into very small fragments.

3.3. Molecular Modeling Study of the Interaction Between HSA and Compound 7

Molecular docking technique was further employed to understand the interaction between compound 7 and HSA.

Descriptions of the 3D structure of crystalline albumin have revealed that that HSA comprises three homologous domains (denoted I, II, and III): I (residues 1–195) II (196–383) and III (384–585); each domain has two subdomains (A and B) that assemble to form heart shaped molecule (Figure 11). The principal region of drug binding sites of HSA are located in hydrophobic cavities in subdomain IIA and IIIA, which are corresponding to site I and site II, respectively and tryptophan residue (Trp-214) of HSA in subdomain IIA [30]. There is a large hydrophobic cavity in subdomain IIA to accommodate the compound 7, which play an important role in absorption, metabolism, and transportation of HSA. The results (Figure 12 a&b) revealed that the compound 7 was half-surrounded within subdomain IIA hydrophobic cavity, and it is in close proximity to hydrophobic residues, such as Trp214, Arg2018, Arg222, Ser390, etc., of subdomain IIA of HSA, suggesting the existence of hydrophobic interaction between them. Hence, this finding provides a good structural basis to explain the efficient fluorescence quenching of HSA emission in the presence of the compound 7. Furthermore, there are also a number of weak electrostatic interactions and hydrogen bonds, because several ionic and polar residues in the proximity of the ligand play an important role in stabilizing the molecule *via* H-bonds and weak electrostatic interactions. The results obtained from molecular docking indicated that the interaction between compound 7 and HSA was dominated by hydrophobic forces as well as hydrogen bonds, which was consistent with our experimental results.

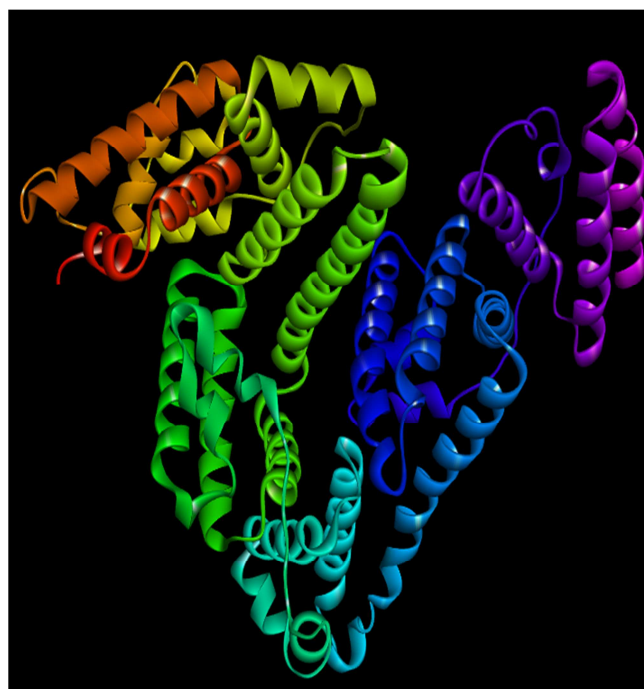


Figure 11. X-ray crystallographic structure of HSA (PDB ID: 1h9z). The domains and subdomains were displayed with different color, the every subdomain and classical binding site were marked in the corresponding location.

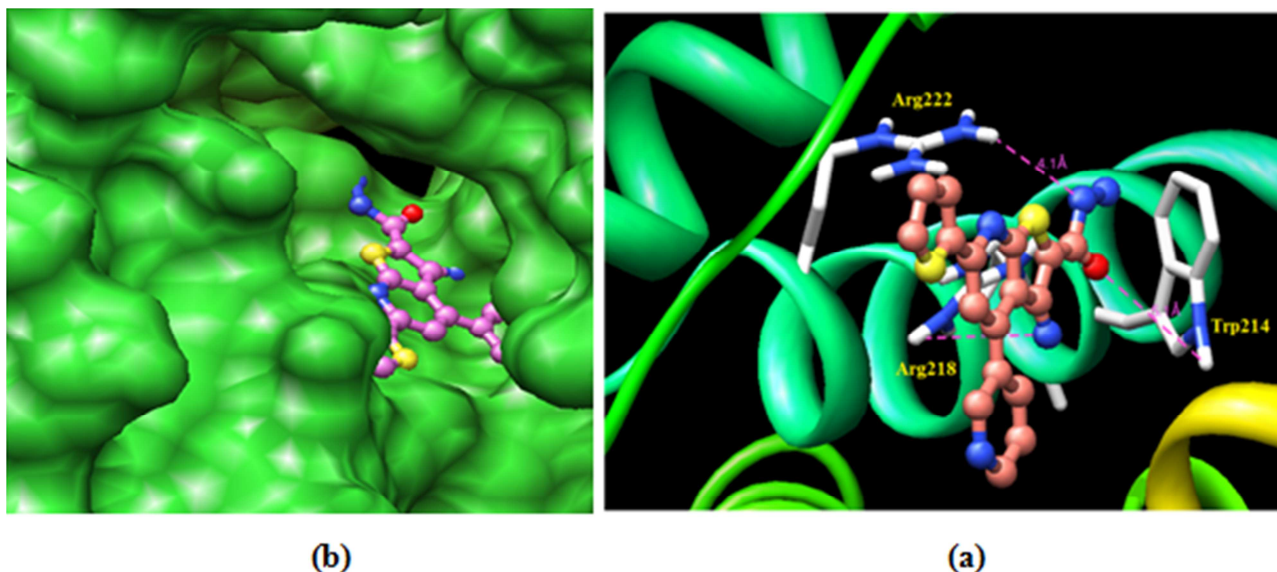


Figure 12. Molecular docked model of (a) The interaction mode between compound 7 (showing stick representation) and HSA (cartoon form) and the green dashed line showing hydrogen bond interaction between them. (b) compound 7 (stick representation) located within the hydrophobic pocket in subdomain IIA of HSA.

4. Conclusion

In the present work, a new series of 3-amino-4-pyridin-3-yl-6-(2-thienyl)thieno[2,3-*b*]pyridine-2-carbohydrazides (7) was synthesized using 4 and 5 with hydrazine hydrate. The interaction between compound 7 and HSA was investigated employing different spectroscopic (fluorescence, CD, FTIR) and molecular docking techniques. The experimental results indicated that the compound 7 binds to HSA with moderate affinity and the intrinsic fluorescence of HSA was quenched through static quenching mechanism. The binding parameters were calculated using the modified Stern-Volmer equation. The thermodynamic parameters, negative value of ΔH , positive value of ΔS and the negative value of ΔG indicate that hydrophobic and hydrogen bonding interactions playing a major role in the binding process located within site I (subdomain IIA). The distance (r) between Trp-214 of HSA and compound 7 was evaluated as $r = 4.1$ nm, in accordance with Förster non-radioactive resonance energy-transfer theory. Furthermore, CD and FT-IR evidences show that the secondary structure of HSA was changed after compound 7 was bound to HSA. The results may provide valuable information to understand the mechanistic pathway of drug delivery and to pharmacological behavior of drug.

List of abbreviations

Humanserumalbumin:(HSA)
 Fluorescenceresonanceenergytransfer:(FRET)
 N'-tetramethylethylenediamine:(TEMED)
 2-mercaptoethanol:(MPE)
 SodiumDodecylSulphate:(SDS)
 Fourier-transformInfrared:(FTIR)
 UltraViolet-visible spectrophotometer:(Uv-vis)
 Proteindatabank:(PDB)

Circulardichroism:(CD)
 Tryptophan:(Trp)

References

- [1] Miniyar P. B., Mokale S. N., Makhija S. J., *Arab. J. Chem.* 10 (2017) 41.
- [2] Cynamon, M. H., Klemen, S. P., Chou, T. S., Gimi, R. H., Welch, J. T., *J. Med. Chem.* 35 (1992) 1212.
- [3] José C., Arthur B., Neira G., Juan R., Rosario R., Abraham V., Robert G., Jaime C., *Bioorg. Med. Chem.* 19 (2011) 2023.
- [4] Nakane T., Kazuo T., Masayuki H., Toshiharu T., Isao Y., Toshihiro F., Youichi T., Yasuaki N., Kazuo H., Tsutomu T., Nobu A., Mitsune T., Kazuma O., Akio U., Toru M., Akihisa K., *J. Infec. Chemotherapy* 21 (2015) 16.
- [5] Duranton F., Cohen G., De Smet R., Rodriguez M., Jankowski J., Vanholder R., Argiles A., *J. Am. Soc. Nephro.* 23 (2012) 1258.
- [6] Fanali G., di Masi A., Trezza V., Marino M., Fasano M. Ascenzi, P., *Mol. Aspects Med.* 33 (2012) 209.
- [7] Chi-Ren H., Chih-Hsiang L., Shu-Chen H., Nai-Ching C., Wan-Chen T., Shang-Der C., Yan-Ting L., Yao-Chung C. K. *J. Med. Sci.* 33 (2017), 130.
- [8] Waddhaah M. A., Sartaj T., Mohd A., Farukh, A., Rizwan H. K., *Mol. Omics* 8 (2012) 2424.
- [9] Chuang V. T. G., Kragh-Hansen U., & Otagiri M, *Pharm. Res.* 19 (2002) 569.
- [10] Pace C. N., Vajdos, F., Fee L., Grimsley G., Gray T, *Protein Science* 4 (1995) 2411.
- [11] Stephanos, J. J., *J. Inorg. Biochem.* 62 (1996). 155.
- [12] Trynda-Lemiesz L., Keppler B. K., Koztowski H., *J. Inorg. Biochem.* 73 (1999) 123.

- [13] Lakowicz J. R., Principles of fluorescence spectroscopy, 2nd ed., Plenum Press, New York (1999) pp. 237.
- [14] Förster T., Sinanogl, O., *Modern Quantum Chemistry* 3 (1996) 93, Academic Press, New York.
- [15] Cyril L., Earl J. K. Sperry W. M., *Biochemists Handbook* (1961) 84 E. & F. N. Spon, London.
- [16] Lu, Z. X., Cui, T., Shi, Q. L. Applications of Circular Dichroism and Optical Rotatory Dispersion in Molecular Biology (1987) (1st ed, pp. 79). Science Press.
- [17] Liu J. Q., Tian J. M., Tian X., Hu Z. D., Chen X. G., *Bioorg. Med. Chem.* 12 (2004) 469.
- [18] de Souza G. L. C., de Oliveira L. M., Vicari R. G., Brown A., *J. Mol. Struct.* 22 (2016) 1.
- [19] Ritche D. W., Venkataraman V., *Bioinformatics* 26 (2010) 2398.
- [20] Feng X. Z., Bai C. L., Lin Z., *Anal. Chem.* 26 (1998) 154.
- [21] Silva D., Cortez C. M., Bastos J. C., *Toxicol. Lett.* 147 (2004) 53.
- [22] Zhang Y. Z., Zhou B., Liu Y. X., Zhou C. X., Ding X. L., Liu Y., *J. Fluor.* 18 (2008) 109.
- [23] Ross P. D., Subramanian S., *Biochemistry* 20 (1981) 3096.
- [24] Valeur B., Brochon J. C., *Springer Press*, Berlin (1999) pp. 25.
- [25] Cui F., Fan J., Li J., Hu Z., *Bioorg. Med. Chem.* 12 (2004) 151.
- [26] Ahmad B., Parveen S., Khan R. H., *Biomacromolecules* 7 (2006) 1350.
- [27] Huilun C., Honghao R., Jian Y., Yongxiang Q., Fei W., Jun Y. *J. Envir. Sci. Health* 51: 3 (2015) 154.
- [28] Luz M. M., Moreno-Gordaliza E., Moraleja I., Canas B., Gomez-Gomez M. M., *J. Chromatography A* 1218 (2011) 1281.
- [29] Jesper O., Christian S., Claus L., Niels H. H. H., *Electrophoresis* 23 (2002). 2842.
- [30] Tang J., Luan F., Chen X., *Bioorg. Med. Chem.* 14 (2006) 3210.